Cell Stress and Chaperones (2014) 19:479–491
DOI 10.1007/s12192-013-0474-3

ORIGINAL PAPER

Vitamin D receptor-modulated Hsp70/AT_1 expression may protect the kidneys of SHRs at the structural and functional levels

Isabel Mercedes García · Liliana Altamirano · Luciana Mazzei · Miguel Fornés · Fernando Darío Cuello-Carrión · León Ferder · Walter Manucha

Received: 10 September 2013 / Revised: 22 October 2013 / Accepted: 24 October 2013 / Published online: 13 November 2013

Abstract Previous hypertension studies have shown that low levels of vitamin D are linked to elevated renin–angiotensin system. The heat shock protein 70 regulates signaling pathways for cellular oxidative stress responses. Hsp70 has been shown to protect against angiotensin II-induced hypertension and exert a cytoprotective effect. Here, we wanted to evaluate whether the vitamin D receptor (VDR) associated with Hsp70/AT_1 expression may be involved in the mechanism by which paricalcitol provides renal protection in spontaneously hypertensive rats (SHRs). One-month-old female SHRs were treated for 4 months with vehicle, paricalcitol, enalapril, or a combination of both paricalcitol and enalapril. The following were determined: blood pressure; biochemical parameters; fibrosis; apoptosis; mitochondrial morphology; and VDR, AT_1 receptor, and Hsp70 expression in the renal cortex. Blood pressure was markedly reduced by enalapril or the combination but not by paricalcitol alone. However, VDR activation, enalapril or combination, prevented fibrosis, the number of TUNEL-positive apoptotic cells, mitochondrial damage, and NADPH oxidase activity in SHRs. Additionally, high AT_1 receptor expression, like low Hsp70 expression (immunohistochemical/immunofluorescence studies), was reversed in the renal cortices of paricalcitol- and/or enalapril-treated animals (SHRs), and these changes were most marked in the combination therapy group. Finally, all of the recovery parameters were consistent with an improvement in VDR expression. Data suggest that Hsp70/AT_1 modulated by VDR is involved in the mechanism by which paricalcitol provides renal protection in SHRs. We propose that low AT_1 expression through VDR induction could be a consequence of the heat shock response Hsp70-mediated cell protection.

Keywords Hypertension · Vitamin D receptor · Angiotensin II type 1 receptor · Heat shock protein 70 · Renal cytoprotection

I. M. García · L. Altamirano · L. Mazzei · W. Manucha
Área de Fisiopatología, Departamento de Patología, Facultad de Ciencias Médicas, Universidad Nacional de Cuyo, Mendoza, Argentina

L. Mazzei · F. D. Cuello-Carrión · W. Manucha
IMBECU-CONICET (National Council of Scientific and Technical Research of Argentina), Buenos Aires, Argentina

I. M. García · L. Altamirano
Área de Farmacología, Departamento de Patología, Facultad de Ciencias Médicas, Universidad Nacional de Cuyo, Mendoza, Argentina

L. Ferder
Department of Physiology and Pharmacology, Ponce School of Medicine and Health Sciences, Ponce, Puerto Rico

M. Fornés
IHEM-CONICET (National Council of Scientific and Technical Research of Argentina), Buenos Aires, Argentina

I. M. García
Departamento de Bioquímica y Ciencias Biológicas, Facultad de Química, Bioquímica y Farmacia, Universidad Nacional de San Luis, San Luis, Argentina

W. Manucha (✉)
Área de Fisiología Patológica, Departamento de Patología, Facultad de Ciencias Médicas, Universidad Nacional de Cuyo Centro Universitario, Mendoza 5500, Argentina
e-mail: wmanucha@yahoo.com.ar

Introduction

Hypertension is associated with functional and structural changes including endothelial dysfunction, altered contractility, vascular remodeling, cellular apoptosis, fibrosis, and oxidative stress (Paravicini and Touyz 2006; Touyz and Briones 2011). Indeed, recent evidence indicates that in the

pathogenesis of primary hypertension, the interstitial accumulation of immune cells is associated with increments in oxidative stress and renal angiotensin II (AngII) activity (Quiroz et al. 2012). In the kidney, AngII, via the type 1 (AT_1) receptor, activates several subunits of the membrane-bound multicomponent NADPH oxidase (Montezano and Touyz 2012), and also increases reactive oxidative species (ROS) formation in the mitochondria (Sachse and Wolf 2007). Further, overproduction of ROS has previously been identified as a key component of apoptotic pathways (Franklin et al. 2006). In addition, AngII upregulation stimulates oxidative stress in the proximal tubules of spontaneously hypertensive rats (SHRs) (White and Sidhu 1998), contributing to the development of hypertension-induced tubulointerstitial renal injury (Zhuo et al. 2002). Induction of the stress response includes synthesis of heat shock protein 70 (Hsp70), a molecular chaperone that has a critical role in the recovery of cells from stress and in cytoprotection since it regulates a diverse set of signaling pathways for cellular oxidative stress responses. Of particular interest, a clinical study revealed Hsp70 involvement in the adaptive response of the human kidney to congenital unilateral ureteropelvic junction obstruction (Vallés et al. 2003). More specifically, several models of hypertension are associated with increased susceptibility to environmental stress and increased accumulation of heat shock protein mRNA. Hsp70 polymorphism has been demonstrated when comparing normotensive and hypertensive rats (Lovis et al. 1994). Unprecedented, our laboratory demonstrated that Hsp70 expression protects against AngII-induced hypertension and exerts a cytoprotective effect by downregulating Nox4 (Bocanegra et al. 2010). Previously, Hsp70 induction was suggested as a physiological response to acute hypertension, opening up the possibility that Hsp70 plays a role in protecting the vasculature from damage during hemodynamic stress (Xu et al. 1995). In the contrary, however, Ishizaka el al. demonstrated that an increase in renal Hsp70 expression was dependent on AT_1 receptor activation but not on hypertension per se (Ishizaka et al. 2002). Similarly, we have demonstrated that protection against tubulointerstitial fibrosis by Losartan is independent from changes in blood pressure and includes decreased oxidative stress linked to the upregulation of Hsp70 expression (Manucha et al. 2005).

Finally, both vitamin D deficiency and hypertension are highly prevalent, and there is an emergent interest in the association of vitamin D deficit with the presence of arterial hypertension. Experimental and clinical evidence indicate that vitamin D deficiency and AngII upregulation play a pivotal role in the progression of renal disease associated with hypertension (Forman et al. 2010; Yang et al. 2012). The pleiotropic actions of vitamin D and its analogues are mediated by the vitamin D receptor (VDR), a ligand-dependent transcription factor that belongs to the steroid nuclear receptor gene family (Dusso and Brown 1998; Rachez and Freedman 2000). Furthermore, VDR activators have not only suppressant effects on the renin–angiotensin system (RAS) but also anti-inflammatory and anti-fibrotic ones (Husain et al. 2009; Husain et al. 2010; Li and Batuman 2009). Thus, calcitriol protects renovascular function in hypertension by downregulating AT_1 receptors and reducing oxidative stress (Dong et al. 2012).

Previously, we have demonstrated that paricalcitol (19-nor-1, 25-dihydroxyvitamin D_2, an inducer of vitamin D receptors) was able to ameliorate renal interstitial fibrosis in obstructive nephropathy by means of a possible AT_1 receptor-dependent protective effect that occurs at the mitochondrial level (García et al. 2012).

The present study was performed to evaluate whether VDR associated with Hsp70/AT_1 expression may be involved in the mechanism by which paricalcitol provides renal protection in SHRs. Also, we discuss the possibility that decreased AT_1 expression through VDR induction could be a consequence of the heat shock response Hsp70-mediated cell protection.

Materials and methods

All of the experimental procedures of this study were previously approved by the Laboratory Animal Ethical Committee of the School of Medicine, Cuyo University, Mendoza (IACUL A5780-01). The experiments were conducted in accordance with the guidelines of the Committee of Ethical Animal Experimentation of Argentina as well as with those of the Office of Extramural Research, National Institutes of Health, US Department of Health and Human Services.

Animals and treatment

One-month-old female SHRs were randomized into four groups ($n=10$) and treated, respectively, with vehicle (SHR; 100 μl of propylene glycol/day, i.p.), paricalcitol (SHR+Pari; at 30 ng/kg/day, in 100 μl of propylene glycol, i.p.; provided by Abbott Laboratories), enalapril (inhibitor of the angiotensin-converting enzyme) (SHR+Ena; 20 mg/kg/day, dissolved in drinking water), or paricalcitol and enalapril in combination (SHR+Pari+Ena). The blood pressure of these rats was taken weekly using the CODA tail-cuff blood pressure system (Kent Scientific Corporation). At the end of the treatment (120 days), the animals were sacrificed by exsanguination. The serum was collected for biochemical parameters measurement. The kidneys were removed to be weighed and then evaluated.

Biochemical parameters

The serum concentrations of urea, calcium, phosphorus, and creatinine were determined using colorimetric assays (Sigma kits). Parathyroid hormone (PTH) levels were determined by ELISA. All parameters were measured at the Mega Diagnostic Center of Mendoza (Argentina Biochemical Foundation).

Histological studies

Renal cortex sections were fixed in 10 % phosphate-buffered formalin (pH=7.1) for 24 to 48 h before being embedded in paraffin and serially sectioned (5 μm) on a microtome (Leica). Paraffin sections were stained with Masson's trichrome. For this protocol, renal cortex sections were treated sequentially with Weigert's iron hematoxylin solution for 10 min, Biebrich scarlet–acid fuchsin solution for 2 min, phosphotungstic acid/phosphomolybdic acid for 10 min, and aniline blue for 5 min. Tissue was destained in 1 % acetic acid for 2 min, dehydrated through graded ethanol to xylene, and mounted for examination by light microscopy (Masson 1929).

Morphometric evaluation of interstitial fibrosis

For all morphologic evaluations, the observer was blinded to the origin of the histological sections. A standard point counting method (Hruska et al. 2000; Morrissey et al. 2002) was used to quantitate the fibrosis of the renal interstitium. The fibrosis of the renal cortical interstitium was determined as previously reported (García et al. 2012), and the results were expressed as a percentage of the measured area.

Identification of cellular apoptosis: the TUNEL technique

After the digesting and quenching steps, equilibration buffer was applied directly to the sections, and working-strength TdT enzyme was then applied directly. A biotin-conjugated anti-digoxigenin antibody (Sigma) was used. Then, the sections were incubated with biotinylated anti-mouse IgG (Dako, Carpinteria, CA, USA) at 1:100 dilution for 45 min in order to perform reverse transcription and later with peroxidase-labeled streptavidin–biotin complex/HRP, Dako) at 1:100 dilution for 45 min. After a brief wash (in 3,3′-diaminobenzidine tetrahydrochloride [0.5 mg/ml]/H_2O_2 [0.01 %]), a chromogen substrate, was incorporated. For positive controls, sections from involuting prostates were used (n=2). For the quantification of apoptotic epithelial cells in cross-sectioned cortex areas, ten consecutive fields were randomly selected and were evaluated at ×400 on a 10×10 grid, using an image analyzer.

Electron microscopy

Immediately on being separated from organs, the tissue samples were fixed by immersion in a fixative solution (1:10). The fixative solution was formulated by diluting 1 phosphate saline buffer (PBS) tablet, following the manufacturer instructions, in 200 ml of double distilled water and 2 % glutaraldehyde (v/v), 2 % of fresh p-formaldehyde (v/v), and 2 % of picric acid as saturated solution. After 2 h at room temperature, the samples were reduced and placed in an OsO_4 solution overnight at 4 °C. The next day, the samples were dehydrated in alcohol-acetone grading up to 100 % and embedded in Epon 812 (Sigma). Ultrathin sections were obtained with an Ultracut microtome (Leitz) and stained with lead citrate and uranyl using conventional staining methods. Observations were made and micrographs created using a Zeiss 900 microscope.

Immunohistochemical studies

Kidney paraffin sections (5–6 μm thickness) were dewaxed in xylol, rehydrated, and incubated with 3 % H_2O_2 for 30 min to quench endogenous peroxidase activity. After washing in Tris-buffered saline (0.05 M Tris–HCl, 0.15 M NaCl) pH 7.6 and non-specific blocking with 10 % bovine serum albumin for 30 min at room temperature, the sections were immunostained to reveal VDR, AT_1, and Hsp70. Antibodies applied were mouse monoclonal antibody against VDR (D-6), rabbit polyclonal antibody against Hsp70 (H-300), and rabbit polyclonal antibody against AT_1 (306) (Santa Cruz Biotechnology, Inc.), diluted at 1:500. A commercial immunoperoxidase kit was used (Dako EnVision, Dako Corporation, Carpinteria, CA, USA). The positive reaction was evaluated considering the specific location of immunostaining (renal structure and cell compartment: nucleus, cytoplasm, membrane) and the intensity of the immunoreaction. The negative controls included tissues unexposed to primary antibodies as well as tissues exposed to control immunoglobulin G. The positive controls were human breast cancer biopsy samples.

Immunofluorescence confocal microscopy

The kidneys were washed twice with PBS, placed in isopentane, and stored at −70 °C. Tissue sections (10 μm) were obtained by using a cryostat. Section gelatinized and fixed by paraformaldehyde buffer overnight at 4 °C. After the fixation procedure, they were cryoprotected in a PBS solution supplemented with 0.9 mol/l sucrose overnight at 4 °C. After neutralization with NH_4Cl buffer, the sections were permeabilized for 45 min with saponin 0.05 % PBS (pH=7.4) before being incubated overnight with the following primary

Table 1 Blood pressure and biochemical parameters in SHRs: *Paricalcitol* and *Enalapril's* effects

	SHR	SHR+Pari	SHR+Ena	SHR+Pari+Ena
MBP (mmHg)	190±9	175±10	120±8**	110±9**
Urea (mg/dl)	45±1	41±1*	39±2*	36±2**
Creatinine (mg/dl)	0.65±0.02	0.60±0.01*	0.59±0.05*	0.55 ±0.02**
Calcium (mg/dl)	6.3±0.05	6.0±0.03*	5.9±0.02*	5.65±0.01**
Phosphorus (mg/dl)	7.2±0.20	7.10±0.30*	7.05±0.30*	6.75±0.20**
Ca x P product (mg^2/dl^2)	43±1	38±1*	38.5±1.1*	35±1.3**
PTH (pg/ml)	51±1	46±1*	45±2*	32±3**

Mean blood pressure (MBP) was significantly reduced in enalapril-treated rats (SHR+Ena, $^{**}P<0.01$) as well as in enalapril/paricalcitol-treated rats (SHR+Pari+Ena, $^{**}P<0.01$), but paricalcitol alone (SHR+Pari, P=NS) did not control MBP. In addition, enalapril or paricalcitol (SHR+Ena or SHR+Pari, $^{*}P<0.05$) contributed to improving renal function as well as biochemical parameters. Unexpectedly, the combined treatment (SHR+Pari+Ena, $^{**}P<0.01$) was better at reducing all of the serum parameters evaluated. Results are mean±S.E.M.; $n=10$

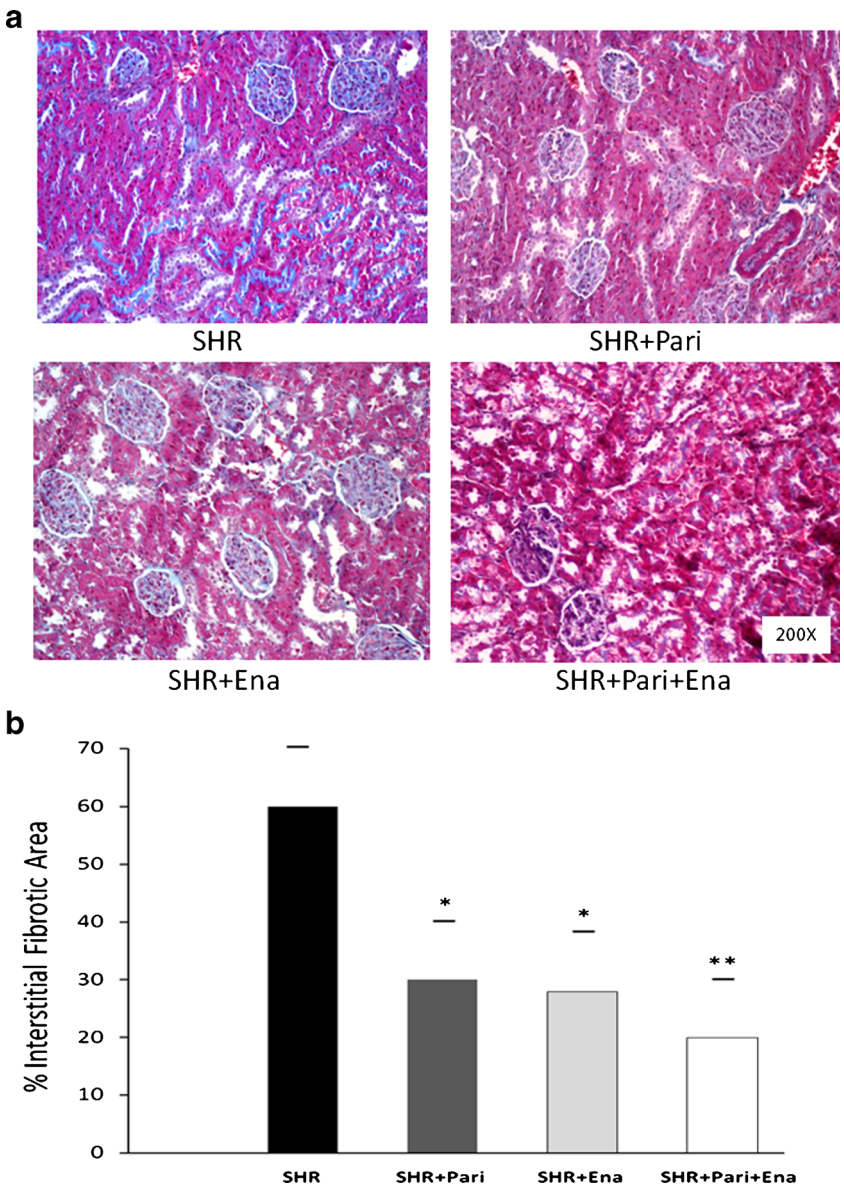

Fig. 1 Masson's trichrome-stained sections of the SHR kidney cortices. **a** Kidney cortex from vehicle-treated rats (*SHR*); kidney cortex from paricalcitol-treated rats (*SHR+Pari*); kidney cortex from enalapril-treated rats (*SHR+Pari+Ena*); and kidney cortex from combined-treatment rats (*SHR+Pari+Ena*). Magnification, ×200. **b** Representative graphics of Masson's trichrome quantification. The interstitial fibrotic area of the SHR kidneys revealed a significant expansion of the interstitial space compared to the cortical areas of the SHR+Pari and SHR+Ena groups, respectively (*SHR* vs. *SHR+Pari* and *SHR* vs. *SHR+Ena*; $^{*}P<0.05$). Also, no differences were observed in the cortices of the animals in the SHR paricalcitol-treated group compared to the animals on the SHR enalapril-group (*SHR+Pari* vs. *SHR+Ena*; P=NS). Highlights in the SHR+Pari+Ena group were that the expansion of the interstitial space was significantly decreased compared to that of the SHR group (*SHR+Pari+Ena* vs. *SHR*; $^{**}P<0.01$). Results are mean±S.E.M.; $n=10$

antibodies: monoclonal anti-Hsp70 (1:100) (Sigma Aldrich), monoclonal anti-VDR (1:100) (Santa Cruz Biotechnology), and polyclonal anti-AT_1 (1:100) (Santa Cruz Biotechnology). Secondary antibodies were goat anti-rabbit IgG antibody, Cy2 conjugated (1:750) and donkey anti-mouse IgG antibody, Cy3 conjugated (1:750). After being washed, the tissues were stained with Hoechst 33342 (10 nM) for 5 min. The coverslips were mounted in Fluoroshield solution (Sigma Aldrich) for confocal microscopy. Confocal immunofluorescence images were taken using FV10-ASW 1.7 Viewer software with the Olympus IX81 microscope. Images were processed and analyzed using Macbiophotonics ImageJ.

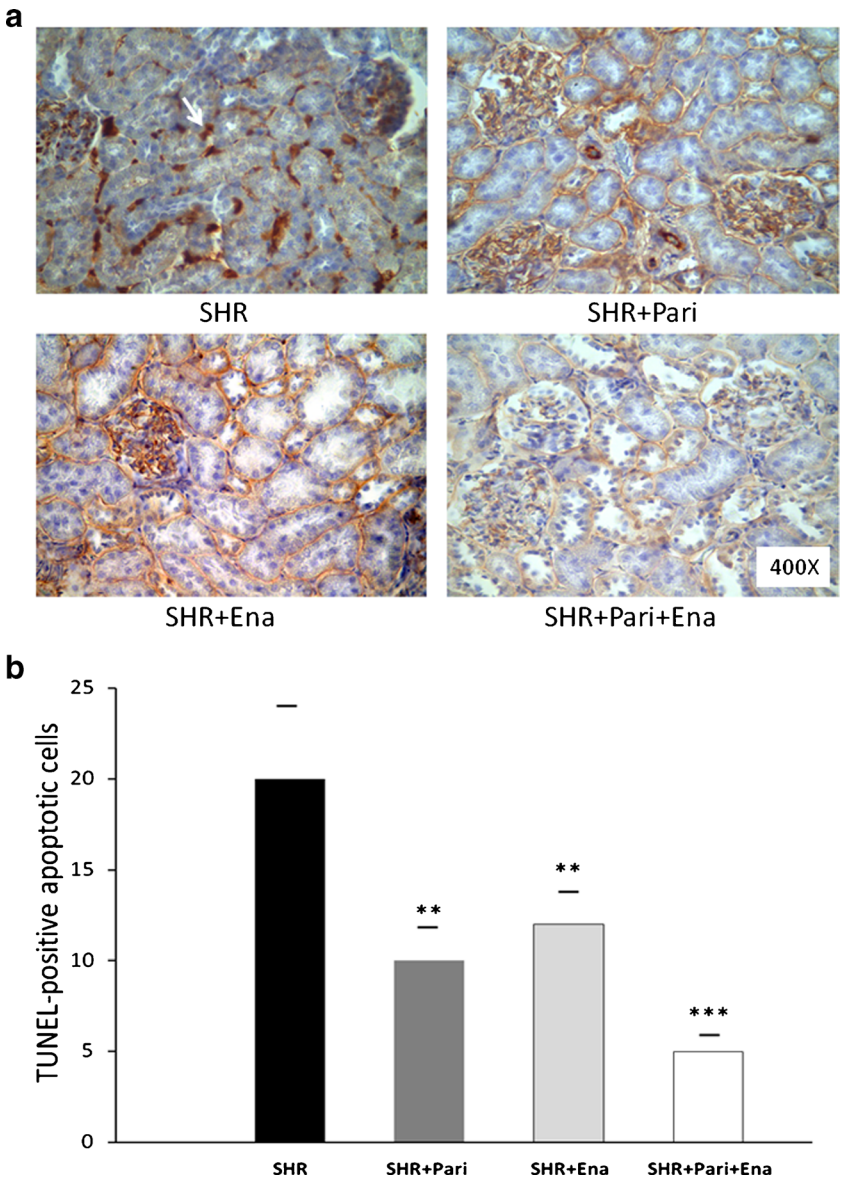

Fig. 2 Histologic sections of the cortices of kidneys following hypertension for 120 days: *Paricalcitol* and *enalapril*'s cytoprotective effect. **a** Localization of apoptotic nuclei by TdT-uridine-nick-end-labeling technique. Apoptotic nuclei appear as heavy brown-stained nuclei in tubule epithelial cells (*arrow*). Following 120 days of hypertension in the renal cortex (*SHR*), apoptotic nuclei appear as heavy brown-stained nuclei in collecting ducts and in lesser proportions in proximal tubules, whereas there is a slight increase in apoptotic cells in epithelium from collecting ducts and proximal tubules in the SHR+Pari and SHR+Ena group's kidney cortices. To highlight, apoptotic cells were rarely seen in the tubule epithelial cells of the combined-treatment (*SHR+Pari+Ena*) group. Magnification ×400. **b**. Quantification of apoptotic epithelial cells in the cortices (seen in cross-section). There was a decreased number of TUNEL-positive nuclei in the tubular epithelial cells of the cortices from the paricalcitol-treated (*SHR+Pari*) and enalapril-treated animals (*SHR+Ena*), respectively, compared to what was seen in SHRs without treatment, $^{**}P<0.01$. Interestingly, in the cortices from the paricalcitol/enalapril-treated animals (*SHR+Pari+Ena*), the number of TUNEL-positive apoptotic cells was significantly lower than what was found in the vehicle-treated animals (*SHR*), $^{***}P<0.001$. No differences were observed in the cortices of the paricalcitol-treated animals compared to those of the enalapril-treated animals (SHR+Pari vs. SHR+Ena; P=NS). Each *bar* represents mean±S.E.M.; $n=10$

NADPH activity assay

NADPH oxidase activity was measured in mitochondrial fractions of the renal cortex using the Luminol (5-amino-2, 3-dihydro-1, 4-phthalazine, Sigma-Aldrich) technique. Mitochondrial isolation from tissue as well as purity was performed according to our previous reports (García et al. 2012). The values were expressed as relative fluorescence units (RFU) per microgram of protein and per min of incubation.

Statistical analysis

The results were assessed using one-way analysis of variance (ANOVA) for comparisons among groups. Differences between groups were determined using the Bonferroni post-test. A $P<0.05$ was considered to be significant. Results are given as mean±standard error medium (S.E.M.). Statistical tests were performed using GraphPad InStat version 3.00 for Windows 95 (GraphPad Software, Inc., La Jolla, CA, USA).

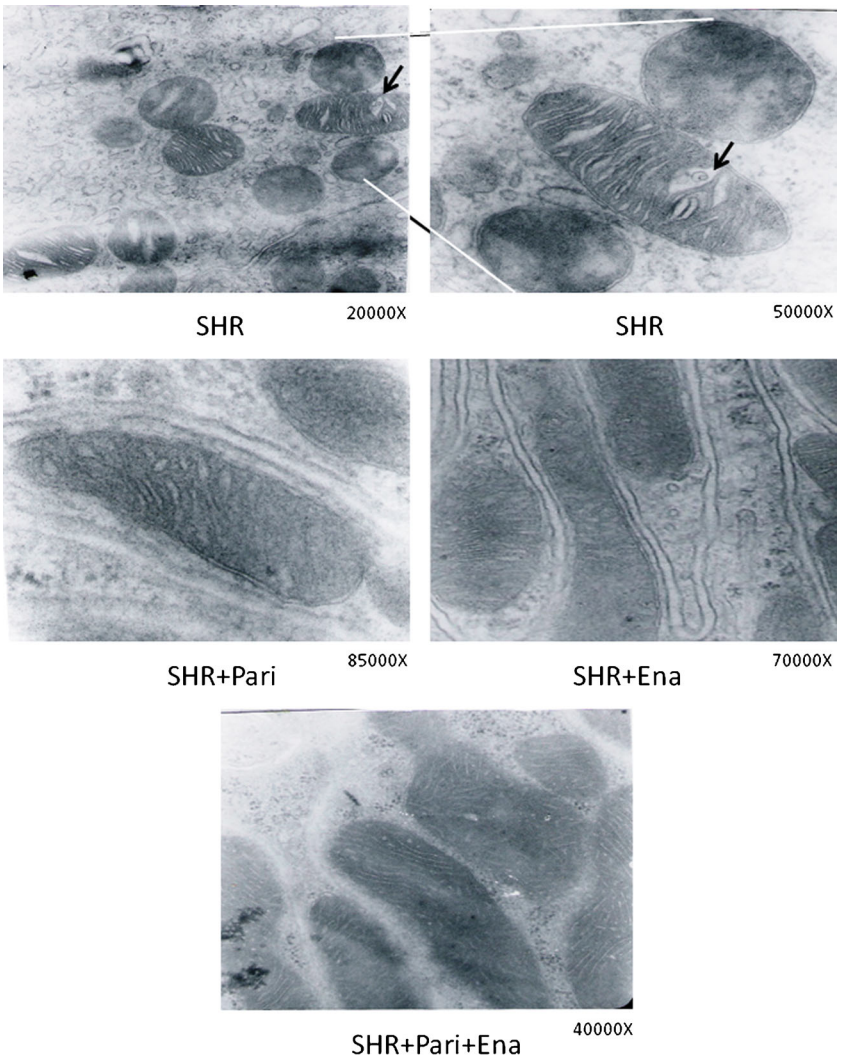

Fig. 3 Electron microscopy study of the cortex of the kidney following hypertension for 120 days: the effect of *Paricalcitol* and *Enalapril* treatment. The *upper row* corresponds to EM obtained from the cortical cortex of an untreated hypertensive kidney (*SHR*). The *second row* corresponds to EM obtained from the cortical cortex of a hypertensive kidney paricalcitol-treated (*SHR+Pari*), and from the cortical cortex of a hypertensive kidney enalapril-treated (*SHR+Ena*). *Lower row* correspond to EM obtained from the cortical cortex of a hypertensive kidney paricalcitol–enalapril-treated (*SHR+Pari+Ena*). Thin sections of renal cortices from SHRs showed altered mitochondria. At high magnification (the *area between the lines*), some of the changes were clearly detected as increased spaces between mitochondrial cristae, vacuoles (*arrows*), and condensation of intramitochondrial material. Conversely, when the animals were treated with paricalcitol (*SHR+Pari*) or enalapril (*SHR+Ena*), mitochondrial swelling between the cristae was less frequent as were intramitochondrial vacuoles. In addition, mitochondria appeared normal when animals were treated with both drugs (*SHR+Pari+Ena*)

Results

Blood pressure and serum chemistries

Mean blood pressure (MBP) was well-controlled in enalapril-treated rats (SHR+Ena) as well as in enalapril/paricalcitol-treated rats (SHR+Pari+Ena), but paricalcitol alone (SHR+Pari) did not control MBP (Table 1). The treatment with enalapril or paricalcitol (SHR+Ena or SHR+Pari) ameliorated the deterioration of renal function and improved calcium, phosphorus, calcium-phosphorus product, and PTH levels. Unexpectedly, the combined treatment (SHR+Pari+Ena) was better at reducing all of the serum parameters evaluated.

Paricalcitol and enalapril's effects on interstitial fibrosis, apoptosis, and ultra-structural mitochondrial changes during hypertension

Figure 1a shows the degree of tubulointerstitial fibrosis in the renal cortices of SHR kidneys that were subjected to treatment either with vehicle or with drugs. In comparison to those of the SHRs, kidneys subjected to enalapril or paricalcitol showed lower collagen accumulation in the expanded interstitium along with cellular interstitial infiltrates in the cortex. In addition, the kidneys from SHRs that underwent combined treatment (SHR+Pari+Ena) had less interstitial collagen deposition compared to what was seen in the kidneys of SHR+Pari and/or SHR+Ena.

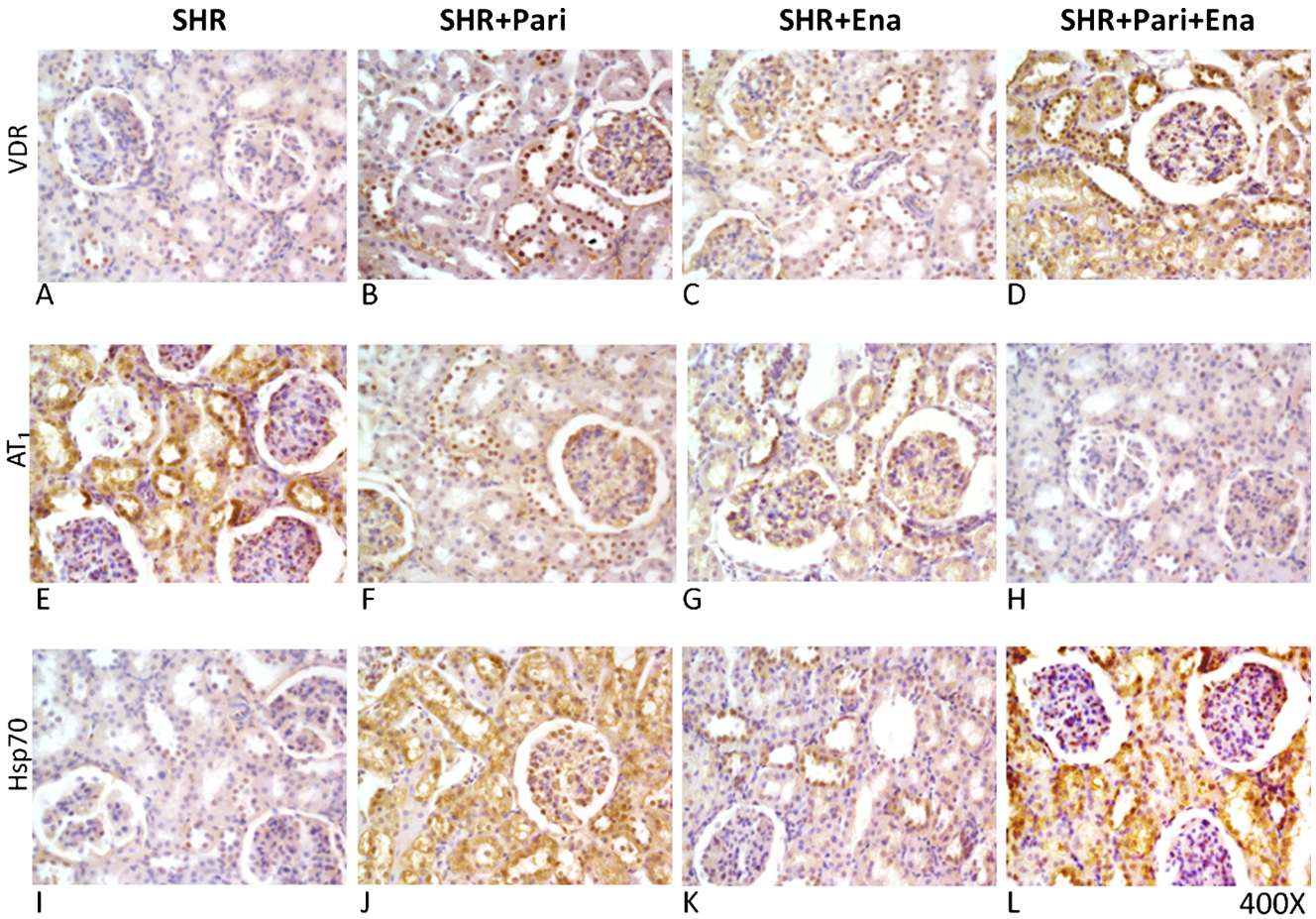

Fig. 4 Histological sections of adult kidney cortices following 120 days of hypertension. In fact, in the SHR rats, the VDR and HSP70 immunostaining (expression) was relatively low, and it was increased following the various treatments in the cytoplasm from tubule epithelial cells (A and I), while, contrarily, AT_1 staining was seen in the same epithelial duct segments (*E*). Conversely, after paricalcitol (*SHR+Pari*) and/or enalapril (*SHR+Ena*) treatment, increased VDR/Hsp70 immunostaining levels were seen in cortex tubule cells compared to SHR vehicle-treated animals (*B*, *J*, *C*, and *K*). In addition, lower AT_1 staining in tubule cells from SHR+Pari and/or SHR+Ena compared to cells from SHR vehicle-treated animals were demonstrated (*F* and *G*). Moreover, after the administration of paricalcitol/enalapril , a greater increase in VDR/Hsp70 immunostaining levels were seen in cortex tubule cells compared to what was seen in the vehicle-treated SHRs (*D* and *L*). Finally, a very low level of AT_1 staining in the tubule cells from the SHR+Pari+Ena group was seen compared to cells from vehicle-treated SHRs (H). Magnification, ×400

The interstitial fibrotic area of the SHRs revealed a twofold expansion of the interstitial space compared to those of the SHR+Pari and SHR+Ena groups, respectively (60±10 vs. 30±11 % and 60±10 vs. 28±10 %; $P<0.05$, $n=10$). In the

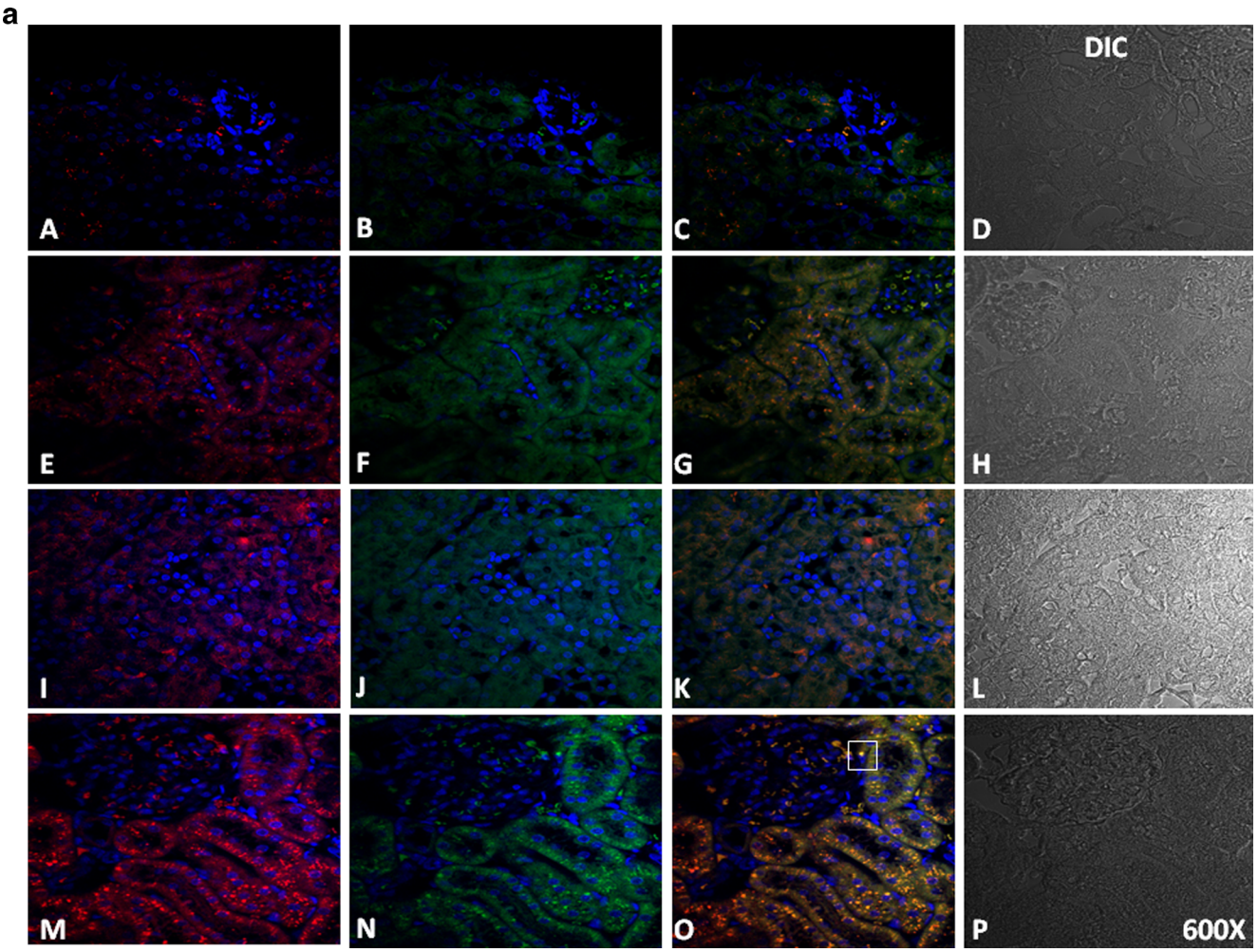

Fig. 5 **a** Immunofluorescence/cytochemical localization of VDR and Hsp70 in kidney cortices from drug-treated or vehicle-treated rats. Renal cortex tissues were double labeled with antibodies against VDR and Hsp70, followed by antirabbit fluorescein isothiocyanate-conjugated and antimouse Rhodamine Red X-conjugated secondary antibodies. Hoechst 33342-stained nucleus (*blue*). Additionally, differential interference contrast (*DIC*) microscopy was performed. Images are representative of five different experiments. In the SHR+Pari and SHR+Ena groups, tubule epithelial cells slight VDR (*E* and *I*) and moderate Hsp70 staining (*F* and *J*) were identified as being related to SHRs in the cytosol, and the overlap between these proteins was poor (*G* and *K*) (VDR *red* and Hsp70 *green*). Conversely, in SHRs, low VDR expression (*A*) appears in the tubule epithelial cells, and Hsp70 becomes less prominent in the cytosol and membrane (*B*), as well; the merged image showed no colocalization (*C*). Surprisingly, after combined drugs administration to SHR (SHR+Pari+Ena), greater immunoreactive VDR (*red* in *M*) and higher Hsp70 (*green* in *N*) in the cytosol and the membrane of epithelial tubule cells were seen in the merged image (*O*). In addition, merged image showed some colocalization (*squares* in *O*, *yellow*). Magnification, ×600. **b** Immunofluorescence/cytochemical localization of VDR and AT_1 in kidney cortices from drug-treated or vehicle-treated rats. Renal cortex tissues were double-labeled with antibodies against VDR and AT_1 followed by antirabbit fluorescein isothiocyanate-conjugated and antimouse Rhodamine Red X-conjugated secondary antibodies. Hoechst 33342 stained the nucleus (*blue*). Additionally, differential interference contrast (DIC) microscopy was performed. Images are representative of five different experiments. In the SHR+Pari and SHR+Ena groups, tubule epithelial cells moderate VDR (*E* and *I*) and low AT_1 staining (*F* and *J*) were identified as being related to SHRs, and the overlap between these proteins was poor (*G* and *K*) (VDR, *red*, and AT_1, *green*). Conversely, in SHRs, low VDR expression (*A*) appears in the tubule epithelial cells, and AT_1 becomes more prominent in the cytosol and the membrane (*B*); the merged image showed some colocalization (*squares* in *C*, *yellow*). Unexpectedly, after the administration of the combination of drugs (SHR+Pari+Ena), greater immunoreactive VDR (*red* in *M*) and very low AT_1 (*green* in *N*) in the cytosol of epithelial tubule cells can be seen in the merged image (*O*). Magnification, ×600. **c** Immunofluorescence/cytochemical localization of VDR and Hsp70 in SHR cortex kidneys from combined treatment. Renal cortex tissues were double-labeled with antibodies against VDR and AT_1 followed by antirabbit fluorescein isothiocyanate-conjugated and antimouse Rhodamine Red X-conjugated secondary antibodies. Hoechst 33342-stained nucleus (*blue*). Additionally, differential interference contrast (DIC) microscopy was performed. After 120 days of combined drugs administration to SHR (SHR+Pari+Ena), greater immunoreactive VDR (*red* in *M*) as well higher Hsp70 (*green* in *N*) in cytosol and membrane of epithelial tubule cells were shown. Possible nuclear and cytoplasmatic colocalization was demonstrated in the overlay image. Magnification ×600

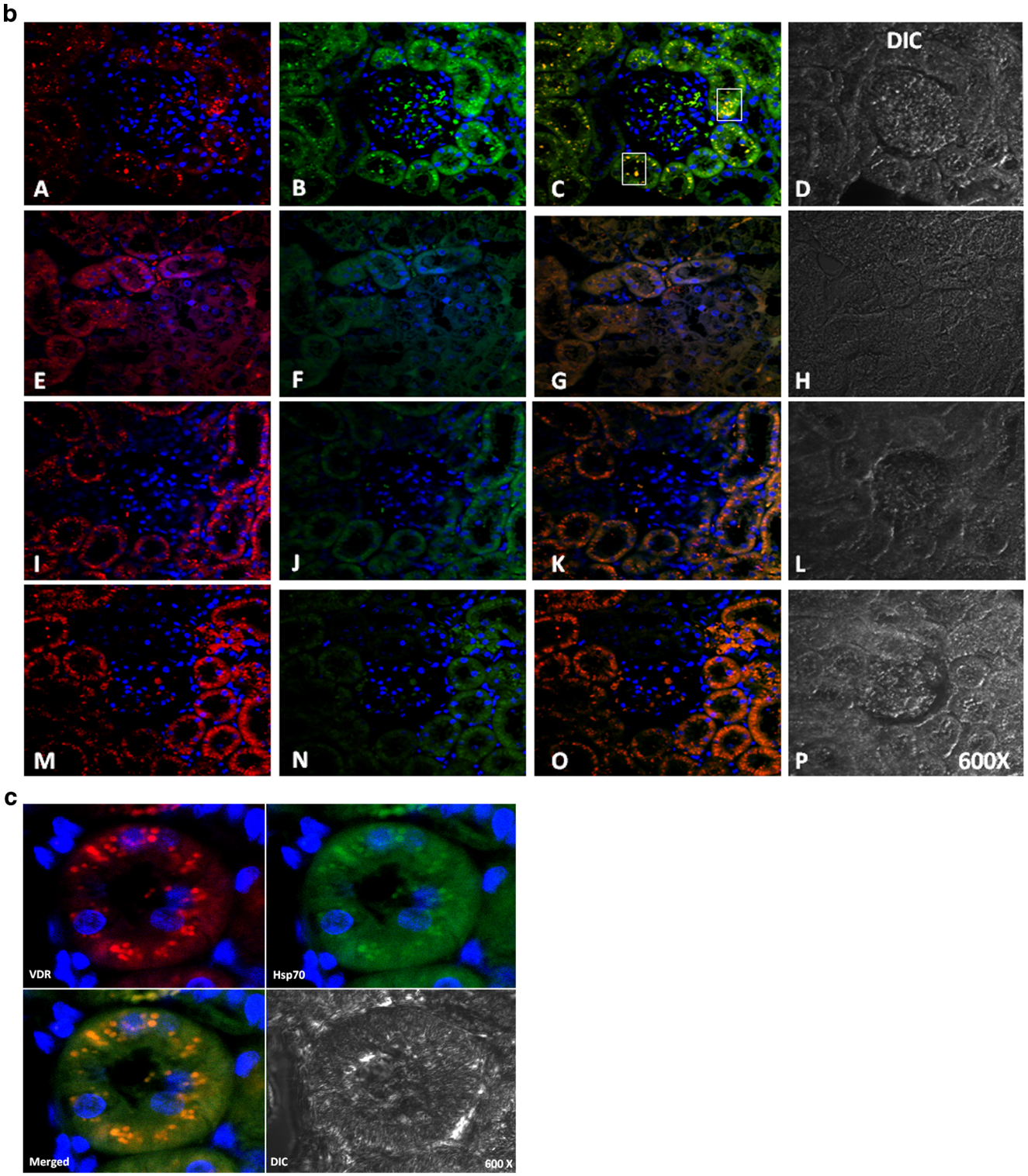

Fig. 5 (continued)

SHR+Pari+Ena group, the expansion of the interstitial space was significantly decreased in relation to that of the SHRs (20±10 vs. 60±10 %; $P<0.01$, $n=10$) (Fig. 1b).

Figure 2a shows an increased number of TUNEL-positive apoptotic cells in tubular epithelial cells from the SHRs compared to those of the SHR+Pari and SHR+Ena groups, respectively (20±4 vs. 10±2 and 20±4 vs. 12±2; $P<0.01$, $n=10$). Interestingly, the number of TUNEL-positive apoptotic cells in the SHR+Pari+Ena group was significantly lower than the number found in the SHR+Pari or SHR+Ena groups,

respectively (5±1 vs. 10±2 and 5±1 vs. 12±2; $P<0.01$, $n=10$). Consistently, in the SHR+Pari+Ena group, the number of TUNEL-positive apoptotic cells was significantly decreased in relation to that of the SHRs (5±1 vs. 20±4 %; $P<0.001$, $n=10$) (Fig. 2b).

Figure 3 shows the results of the electron microscopy study. The architecture of the renal tissue obtained from the SHRs was composed of disorganized cortical tubules, and the cellular structure was also altered (Fig. 3a). These cells contained several vacuoles of different sizes, mitochondria with cristae that were separated (arrow in SHR) by increased spaces between them-some of them containing vacuoles and dense bodies surrounded by membranes. When animals were treated with paricalcitol and/or enalapril (SHR+Pari and/or SHR+Ena), the space between cristae was less notable and the vacuoles disappeared (Fig. 3b, c). Moreover, when the treatment involved both drugs (SHR+Pari+Ena), the cytoplasm and mitochondria recovered the normal appearance for this type of cell, and in addition, the cortical area of the renal tissue were well-preserved in this condition (Fig. 3d).

Paricalcitol and enalapril's effects on VDR, AT_1, Hsp70 expression, and NADPH activity during hypertension

To establish the protein location and the intensity of the immunoreaction, immunocytochemical, and immunofluorescence analysis was performed. Figures 4 and 5 show the expression of VDR, AT_1, and Hsp70 in the cortices of SHRs and in those from the animals in the SHR+Pari, SHR+Ena, and SHR+Pari+Ena groups. In the renal cortices of 120-day SHRs, low VDR and Hsp70 immunostaining/immunofluorescence (Figs. 4 and 5a) were observed in the epithelial cell cytoplasm. Contrary to this, AT_1 staining was shown in the same epithelial cells from SHRs (Figs. 4 and 5b). Increased Hsp70 immunoreaction in the membranes and cytoplasm of the same tubular epithelial cells was shown in the SHR+Pari and SHR+Ena groups compared to the Hsp70 staining of the SHR vehicle-treated group. In addition, in cross-sections of epithelial cells from the SHR+Pari and SHR+Ena groups, higher VDR staining was shown than was seen in the SHR vehicle-treated group (Figs. 4 and 5a). In contrast, low AT_1 immunoreaction was shown in the membranes of the tubular epithelial cells from the SHR+Pari and SHR+Ena groups (Figs. 4 and 5b). In addition, a greater increase of Hsp70 and VDR immunoreaction in the membranes and cytoplasm of the same tubular epithelial cells was shown in the SHR+Pari+Ena group compared to the Hsp70/VDR staining of the SHR vehicle-treated group (Fig. 5c). At the same time, a lesser AT_1 immunoreaction in the membranes and cytoplasm of the same tubular epithelial cells was shown in the SHR+Pari+Ena group compared to the AT_1 staining of SHR animals (Fig. 5c).

Furthermore, preliminary results by western blotting ($n=3$) support these results (data not shown).

Parallel to this study, Fig. 6 shows, in mitochondrial fractions, that NADPH oxidase activity was significantly greater in the SHRs than it was in the SHR+Pari and/or SHR+Ena groups, respectively (30,000±2,000 vs. 20,000±1,500 and/or 30,000±2,000 vs. 19,000±1,700 RFU/μg prot/min; $P<0.01$, $n=10$). In addition, the NADPH oxidase activity in the SHR+Pari+Ena group was significantly lower than the activity found in the SHR+Pari group and/or the SHR+Ena group, respectively (10,000±1,000 vs. 20,000±1,500 and/or 10,000±1,000 vs. 19,000±1,700 RFU/μg prot/min; $P<0.01$, $n=10$). In consequence, the NADPH oxidase activity in the SHR+Pari+Ena group was also significantly lower than the activity found in the SHRs (10,000±1,000 vs. 30,000±2,000 RFU/μg prot/min; $P<0.001$, $n=10$).

Discussion

Experimental and clinical evidence indicate that low vitamin D levels and the stimulation of the RAS are inversely related and represent a risk factor associated with the pathogenesis of hypertension (Ferder et al. 2013). Suppression of RAS gene expression in the kidney by paricalcitol was proposed (Freundlich et al. 2008). However, whether or not the two systems share a regulatory mechanism remains inconclusive. The present study was performed to evaluate whether VDR associated with Hsp70/AT_1 expression may be involved in the mechanism by which paricalcitol provides renal protection in SHRs.

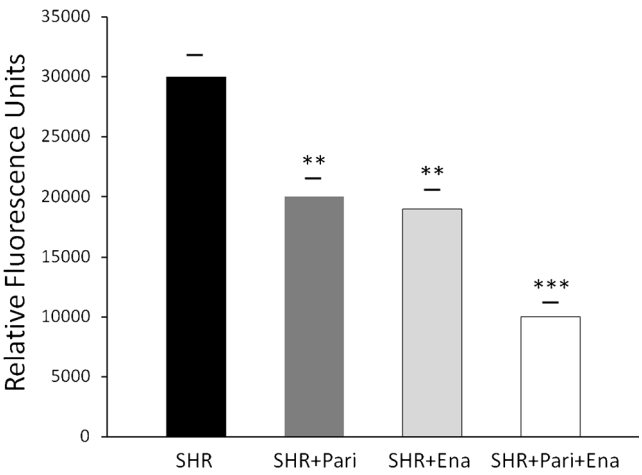

Fig. 6 NADPH Activity in *Mitochondrial* fractions from renal cortices during hypertension. NADPH oxidase activity was decreased in mitochondrial fractions from, respectively, paricalcitol- and enalapril-treated hypertensive kidney cortices (*SHR+Pari* and *SHR+Ena*) compared to untreated *SHR*; $^{**}P<0.01$ for both. While, after paricalcitol and enalapril combined treatment (*SHR+Pari+Ena*), lower NADPH oxidase activity was shown in the mitochondrial fractions from kidney cortices of rats compared to the hypertensive cortices of kidneys from non-treated rats (*SHR*); $^{***}P<0.001$. Each *bar* represents mean±S.E.M.; $n=10$

As expected, blood pressure was well controlled in both the SHR+Ena and the SHR+Pari+Ena groups, but not in the SHR+Pari group. The RAS plays a key role in the pathogenesis of hypertension and is one of the most important targets for drugs. Hence, enalapril (Laragh 1990), caused improvements in the blood pressure of SHRs. On the other hand, and in accordance with a previous report (Bukoski et al. 1993), the induction of VDR failed to reduce blood pressure. However, enalapril or paricalcitol ameliorated the deterioration in renal function as well as improving the biochemical parameters. The combined treatment was better for reducing all of the serum parameters evaluated. Similarly, Finch et al. (2012) demonstrated that while paricalcitol did not improve blood pressure, it may improve renal function and the biochemical parameters in uremic rats, which effect may be amplified when enalapril is added.

In our present study, cellular apoptosis, fibrosis, and oxidative stress were clearly associated with hypertension, as has been the case in previous reports (Paravicini and Touyz 2006; Touyz and Briones 2011). Also, we demonstrated that there was ultrastructural damage at the mitochondrial level in the renal cortices of SHRs. In addition, the presence of high AT_1 and mitochondrial NADPH oxidase activity coupled with low VDR and Hsp70 expression was consistent with the histological and structural changes demonstrated. On the other hand, paricalcitol or enalapril treatment prevented fibrosis, apoptosis, mitochondrial damage, and mitochondrial NADPH oxidase activity in SHR. In accordance, the activation of VDR with calcitriol improves renovascular dysfunction in hypertension by normalizing the expression of AT_1 and prevents the overproduction of ROS (Dong et al. 2012). The silencing of VDR with siRNA displayed the activation of the RAS, and the activation of the VDR resulted in the downregulation of the RAS. ROS generation was inhibited if VDR was activated or if AngII was blocked by Losartan (Rehman et al. 2013). In this context, we show that mitochondrial injury linked to AT_1/VDR uncoupling was improved when paricalcitol, enalapril, or, better still, the combination of both was used. This finding is feasible taking into consideration recent contributions that reported the identification and characterization of a functional mitochondrial RAS (Abadir et al. 2011), the mitochondrial localization of VDR (García et al. 2012 and Silvagno et al. 2010), and ultrastructural mitochondrial improvement as a consequence of recovery in mitochondrial VDR expression linked to poor AT_1 and NADPH oxidase activity during obstructive nephropathy. Moreover, a ligand-independent mitochondrial import of VDR through the permeability transition pore (PTP) was reported (Silvagno et al. 2013); and since functional and structural changes in mitochondria are caused by the opening of the mitochondrial PTP and by the mitochondrial generation of ROS, this finding open new perspectives on PTP function as transporter and on VDR role in mitochondria.

Hsp70 is a molecular chaperone that has a critical role in the recovery of cells from stress (Mayer and Bukau 1998). Consequently, Hsp70 induction was linked to the cytoprotective effect of treatments with paricalcitol, enalapril, and the combination of both in SHRs. Hsp70 interacts with the VDR and plays a role in controlling concentrations of the VDR within the cell (Lutz et al. 2001). Possible colocalization was shown in Fig. 5c. Indeed, Adams et al. (2003) suggested that Hsp70-related intracellular vitamin D-binding proteins act as regulators of vitamin D metabolism. Hsp70 may interact with VDR prior to the activation of the latter by vitamin D (Swamy et al. 1999). Vitamin D has been demonstrated to be a nontoxic inducer of Hsp70 in the rat kidney (Kim et al. 2005). In addition, Hsp70/caveolin-1 interaction has been shown to protect against AngII-induced hypertension and exert a cytoprotective effect by downregulating NADPH (Bocanegra et al. 2010). In fact, caveolin 1 (a 21-kDa cytoskeletal protein) is required for normal renal AT_1 expression (Ishizaka et al. 1998). An interesting avenue of future research would be an assessment of the degree of interaction between the Hsp70, caveolin 1, and AT_1 proteins associated with VDR expression in SHRs.

Collectively, Hsp70 could serve as a cellular intermediary in VDR/AT_1 uncoupling associated with the pathogenesis of hypertension. Future studies are required to clarify the intracellular signaling mechanisms involved in the VDR/Hsp70/AT_1 pathway.

Conclusions and perspectives

The novel proposal presented in this paper is the idea that Hsp70/AT_1 expression modulated by VDR may be involved in the mechanism by which VDR induction provides renal protection in SHRs. Indeed, we discuss the possibility that AT_1-normalized expression through VDR induction could be a consequence of the heat shock response Hsp70-mediated cell protection. According to our knowledge, this is the first study suggesting the involvement of protein Hsp70 as a key factor in the regulatory mechanism between vitamin D receptor and the primary component of the RAS. These concepts could radically alter our understanding of the complex interplay of VDR and RAS during hypertension and similar inflammatory disorders, opening up new avenues of treatment.

Acknowledgements Thanks go to Bob Ritchie of the RCMI Publications Office (5G12-RR003050 [NCRR]/8G12MD007579-27 [NIMHD) for his help in preparing this manuscript. This work was supported by a grant from the National Council of Scientific and Technical Research (CONICET), PIP 2010–2012, awarded to Walter Manucha.

Conflict of interest None.

References

Abadir PM, Foster DB, Crow M, Cooke CA, Rucker JJ, Jain A, Smith BJ, Burks TN, Cohn RD, Fedarko NS, Carey RM, O'Rourke B, Walston JD (2011) Identification and characterization of a functional mitochondrial angiotensin system. Proc Natl Acad Sci U S A 108(36): 14849–14854

Adams JS, Chen H, Chun RF, Nguyen L, Wu S, Ren SY, Barsony J, Gacad MA (2003) Novel regulators of vitamin D action and metabolism: lessons learned at the Los Angeles zoo. J Cell Biochem 88(2): 308–314

Bocanegra V, Manucha W, Peña MR, Cacciamani V, Vallés PG (2010) Caveolin-1 and Hsp70 interaction in microdissected proximal tubules from spontaneously hypertensive rats as an effect of Losartan. J Hypertens 28(1):143–155

Bukoski RD, Li J, Bo J (1993) Effect of long-term administration of 1,25 (OH)2 vitamin D3 on blood pressure and resistance artery contractility in the spontaneously hypertensive rat. Am J Hypertens 6(11 Pt 1):944–950

Dong J, Wong SL, Lau CW, Lee HK, Ng CF, Zhang L, Yao X, Chen ZY, Vanhoutte PM, Huang Y (2012) Calcitriol protects renovascular function in hypertension by down-regulating angiotensin II type 1 receptors and reducing oxidative stress. Eur Heart J 33(23):2980–2990

Dusso AS, Brown AJ (1998) Mechanism of vitamin D action and its regulation. Am J Kidney Dis 32(Suppl 2):S13–S24

Ferder M, Inserra F, Manucha W, Ferder L (2013) The world pandemic of vitamin D deficit could possibly be explained by cellular inflammatory response activity induced by the renin angiotensin system. Am J Physiol Cell Physiol 304(11):C1027–C1039

Finch JL, Suarez EB, Husain K, Ferder L, Cardema MC, Glenn DJ, Gardner DG, Liapis H, Slatopolsky E (2012) Effect of combining an ACE inhibitor and a VDR activator on glomerulosclerosis, proteinuria, and renal oxidative stress in uremic rats. Am J Physiol Renal Physiol 302(1):F141–F149

Forman JP, Williams JS, Fisher ND (2010) Plasma 25-hydroxyvitamin D and regulation of the renin-angiotensin system in humans. Hypertension 55(5):1283–1288

Franklin RA, Rodriguez-Mora OG, Lahair MM, McCubrey JA (2006) Activation of the calcium/calmodulin-dependent protein kinases as a consequence of oxidative stress. Antioxid Redox Signal 8(9–10): 1807–1817

Freundlich M, Quiroz Y, Zhang Z, Zhang Y, Bravo Y, Weisinger JR, Li YC, Rodriguez-Iturbe B (2008) Suppression of renin-angiotensin gene expression in the kidney by paricalcitol. Kidney Int 74(11): 1394–1402

García IM, Altamirano L, Mazzei L, Fornés M, Molina MN, Ferder L, Manucha W (2012) Role of mitochondria in paricalcitol-mediated cytoprotection during obstructive nephropathy. Am J Physiol Renal Physiol 302(12):F1595–F1605

Hruska KA, Guo G, Wozniak M et al (2000) Osteogenic protein-1 prevents renal fibrogenesis associated with ureteral obstruction. Am J Physiol Renal Physiol 279:F130–F143

Husain K, Ferder L, Mizobuchi M, Finch J, Slatopolsky E (2009) Combination therapy with paricalcitol and enalapril ameliorates cardiac oxidative injury in uremic rats. Am J Nephrol 29(5):465–472

Husain K, Suarez E, Isidro A, Ferder L (2010) Effects of paricalcitol and enalapril on atherosclerotic injury in mouse aortas. Am J Nephrol 32(4):296–304

Ishizaka N, Griendling KK, Lasse'gue B, Alexander RW (1998) Angiotensin II type 1 receptor. Relationship with caveolin after initial agonist stimulation. Hypertension 32:459–466

Ishizaka N, Aizawa T, Ohno M, Usui Si S, Mori I, Tang SS, Ingelfinger JR, Kimura S, Nagai R (2002) Regulation and localization of HSP70 and HSP25 in the kidney of rats undergoing long-term administration of angiotensin II. Hypertension 39(1):122–128

Kim YO, Li C, Sun BK, Kim JS, Lim SW, Choi BS, Kim YS, Kim J, Bang BK, Yang CW (2005) Preconditioning with 1,25-dihydroxyvitamin D3 protects against subsequent ischemia-reperfusion injury in the rat kidney. Nephron Exp Nephrol 100(2):e85–e94

Laragh JH (1990) New angiotensin converting enzyme inhibitors. Their role in the management of hypertension. Am J Hypertens 3(11): 257S–265S

Li M, Batuman V (2009) Vitamin D: a new hope for chronic kidney disease? Kidney Int 76(12):1219–1221

Lovis C, Mach F, Donati YR, Bonventre JV, Polla BS (1994) Heat shock proteins and the kidney. Ren Fail 16(2):179–192

Lutz W, Kohno K, Kumar R (2001) The role of heat shock protein 70 in vitamin D receptor function. Biochem Biophys Res Commun 282(5):1211–1219

Manucha W, Carrizo L, Ruete C, Molina H, Vallés P (2005) Angiotensin II type I antagonist on oxidative stress and heat shock protein 70 (HSP 70) expression in obstructive nephropathy. Cell Mol Biol (Noisy-le-grand) 51(6):547–555

Masson PJ (1929) J Techn Methods 12:75–90, AFIP modification

Mayer MP, Bukau B (1998) Hsp70 chaperone systems: diversity of cellular functions and mechanism of action. Biol Chem 379(3): 261–268

Montezano AC, Touyz RM (2012) Oxidative stress, Noxs, and hypertension: experimental evidence and clinical controversies. Ann Med 44(Suppl 1):S2–S16

Morrissey J, Hruska K, Guo G, Wang S, Chen Q, Klahr S (2002) Bone morphometric protein-7 improves renal fibrosis and accelerates the return of renal function. J Am Soc Nephrol 13:S14–S21

Paravicini TM, Touyz RM (2006) Redox signaling in hypertension. Cardiovasc Res 71(2):247–258

Quiroz Y, Johnson RJ, Rodríguez-Iturbe B (2012) The role of T cells in the pathogenesis of primary hypertension. Nephrol Dial Transplant Suppl 4:iv2–iv5. doi:10.1093/ndt/gfs421

Rachez C, Freedman LP (2000) Mechanisms of gene regulation by vitamin D(3) receptor: a network of coactivator interactions. Gene 246:9–21

Rehman S, Chandel N, Salhan D, Rai P, Sharma B, Singh T, Husain M, Malhotra A, Singhal PC (2013) Ethanol and vitamin D receptor in T cell apoptosis. J Neuroimmune Pharmacol 8(1):251–261

Sachse A, Wolf G (2007) Angiotensin II-induced reactive oxygen species and the kidney. J Am Soc Nephrol 18(9):2439–2446

Silvagno F, De Vivo E, Attanasio A, Gallo V, Mazzucco G, Pescarmona G (2010) Mitochondrial localization of vitamin D receptor in human platelets and differentiated megakaryocytes. PLoS One 5(1):e8670

Silvagno F, Consiglio M, Foglizzo V, Destefanis M, Pescarmona G (2013) Mitochondrial translocation of vitamin D receptor is mediated by the permeability transition pore in human keratinocyte cell line. PLoS One 8(1):e54716

Swamy N, Mohr SC, Xu W, Ray R (1999) Vitamin D receptor interacts with DnaK/heat shock protein 70: identification of DnaK interaction site on vitamin D receptor. Arch Biochem Biophys 363(2):219–226

Touyz RM, Briones AM (2011) Reactive oxygen species and vascular biology: implications in human hypertension. Hypertens Res 34(1): 5–14

Vallés P, Jorro F, Carrizo L, Manucha W, Oliva J, Cuello-Carrión FD, Ciocca DR (2003) Heat shock proteins HSP27 and HSP70 in unilateral obstructed kidneys. Pediatr Nephrol 18(6):527–535

White BH, Sidhu A (1998) Increased oxidative stress in renal proximal tubules of the spontaneously hypertensive rat: a mechanism for

defective dopamine D1A receptor/G-protein coupling. J Hypertension 16:1659–1665

Xu Q, Li DG, Holbrook NJ, Udelsman R (1995) Acute hypertension induces heat-shock protein 70 gene expression in rat aorta. Circulation 92(5):1223–1229

Yang L, Ma J, Zhang X, Fan Y, Wang L (2012) Protective role of the vitamin D receptor. Cell Immunol 279(2):160–166

Zhuo JL, Imig JD, Hammond TG, Orengo S, Benes E, Navar LG (2002) Ang II accumulation in rat renal endosomes during Ang II-induced hypertension: role of AT(1) receptor. Hypertension 39:116–121